Supporting Information
Nine pages, four figures, and two tables.
Rates of hydroxyl radical production from transition metals and quinones in a surrogate lung fluid

Jessica G. Charrier[1] and Cort Anastasio[1]*

[1] Department of Land, Air and Water Resources, University of California – Davis

Submitted to Environmental Science & Technology 29 March 2015
Revised Version Submitted 27 June 2015

S1. Chemicals

Sodium chloride (ACS), sodium benzoate (NF/FCC), sodium phosphate dibasic (ACS), potassium phosphate monobasic (ACS), citric acid (99.7%), sulfuric acid (Optima), perchloric acid (Optima) and acetonitrile (HPLC grade) were from Fisher Scientific. Ascorbic acid sodium salt (>99%) was from Fluka. Reduced L-glutathione(>98%), uric acid sodium salt, copper (II) sulfate (99%), phenanthrenequinone (PQN, 99%), 1,2-naphthoquinone (1,2-NQN, 97%), 1,4-naphthoquinone (1,4-NQN, 97%), 1,4-benzoquinone (BQN, 98%) and desferoxamine (95%) were from Sigma Aldrich. para-Hydroxybenzoic acid (99%) and iron (II) sulfate (99.5%) were from Arcos Organics.

S2. Example of Raw ˙OH Data

For some samples we observe a slight lag in initial ˙OH production. Figure S1 shows an example of raw ˙OH concentration measurements for two cases: 1.44 µM of Fe(II) (black), which does not show a lag in ˙OH production, and 4 µM of Cu(II) (grey), which does.

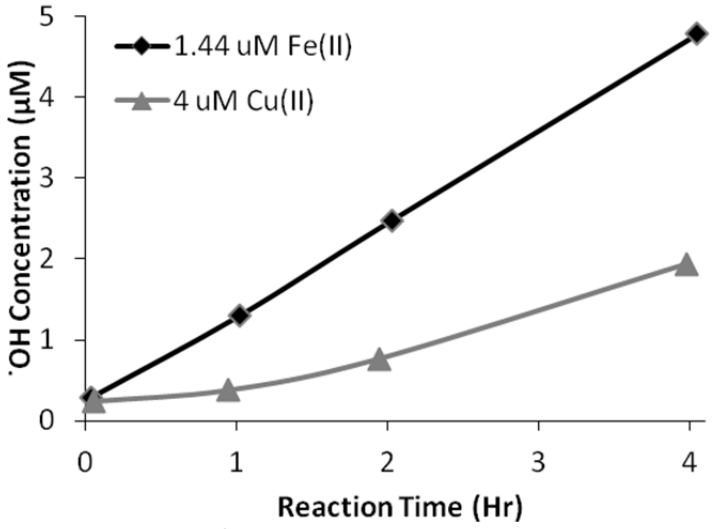

Figure S1. Example of raw ˙OH data. Data are not blank corrected.

S3. Average initial ˙OH rate versus 24 hour integrated total ˙OH

In this work we measure the average rate of ˙OH production by calculating the linear slope of ˙OH concentrations at 0, 1, 2 and 4 hours, as shown in Figure S1. Our previous work measured the integrated total ˙OH produced in 24 hours [1]. We find that ˙OH production over 24 hours is not always linear, thus we cannot reliably calculate that rate of ˙OH production from our previous 24-hour data. Figure S2 shows the difference between these two types of data for Fe(II) and Cu(II) as a function of metal concentration. The total amount of ˙OH formed after 24 hours from our previous work was divided by 24 to estimate the average rate of ˙OH production from 0 to 24 hours in order to compare to the 0 to 4 hour rate in this current work. At low Fe concentrations, ˙OH production is constant over 24 hours and both rates are equal (Figure S1a). At approximately 2000 nM of Fe(II), the rates begin to diverge, indicating that ˙OH production is not constant over 24 hours above this concentration. Cu(II), on the other hand, never shows agreement between the two rate measurements, indicating that ˙OH production from Cu is not constant over 24 hours for any of the concentrations tested. We believe this non-linearity in the production rate stems from ascorbate depletion, thereby reducing the pool of electrons available to form ˙OH. We know that Cu(II) efficiently forms HOOH and ˙OH, which means more electrons will be used up than is the case for Fe, which forms ˙OH but no measurable HOOH, although HOOH is likely present at a very low steady-state concentration throughout. The higher rate for the 0 to 4 hour period indicates that this measure is more robust than the 24-hr total concentration we measured in our past work.

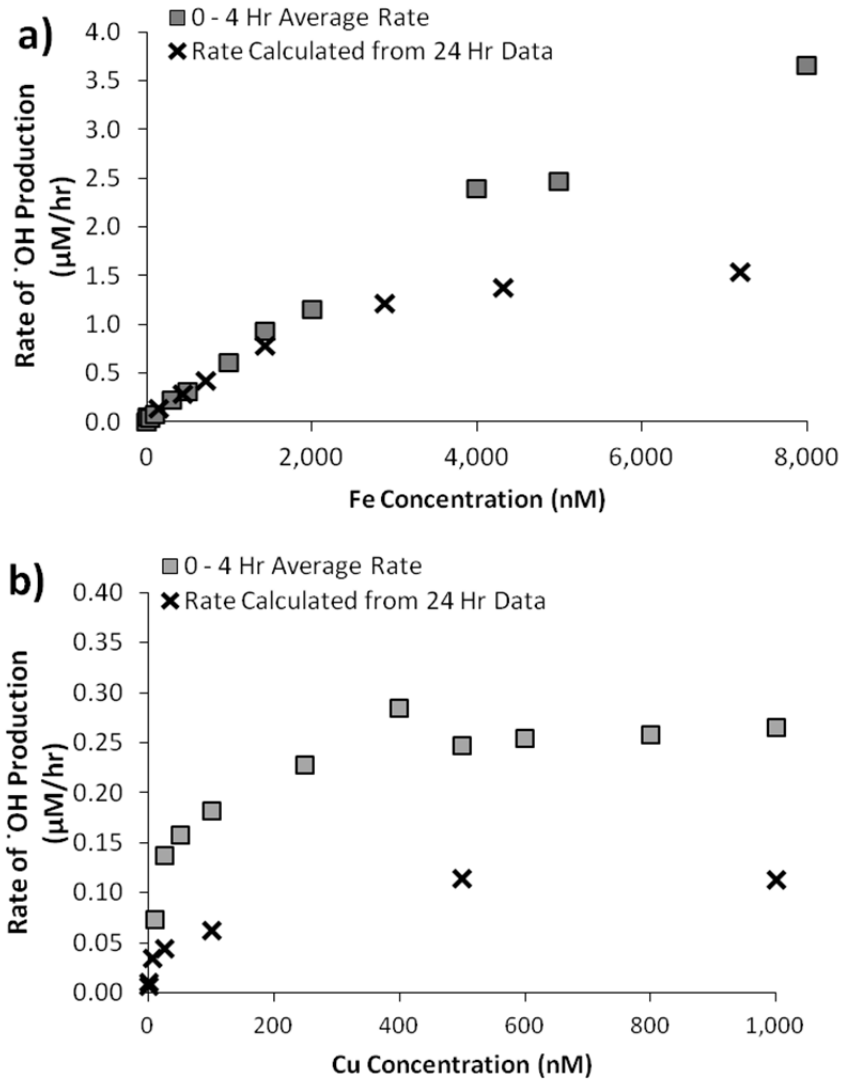

Figure S2. Rate of ˙OH production calculated from 0 to 4 hour data (squares) versus from total 24-hour ˙OH concentrations (crosses) for a) Fe(II) and b) Cu(II). 24-hour data is is from Charrier and Anastasio. [1].

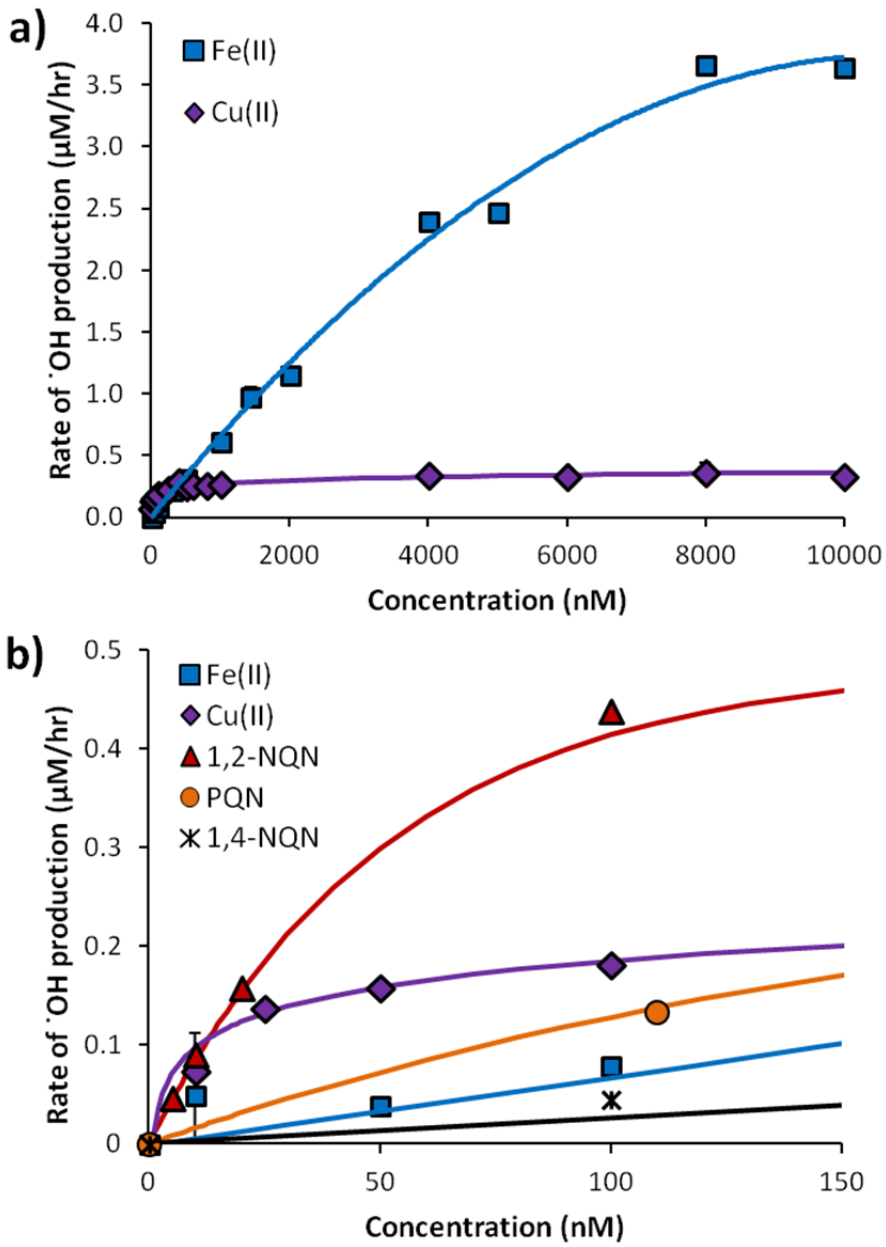

Figure S3. Rate of ˙OH production as a function of concentration of redox-active species. a) zoomed out to higher concentrations of Fe and Cu (0 – 10,000 nM), and b) zoomed in to a lower concentrations (0 – 150 nM).

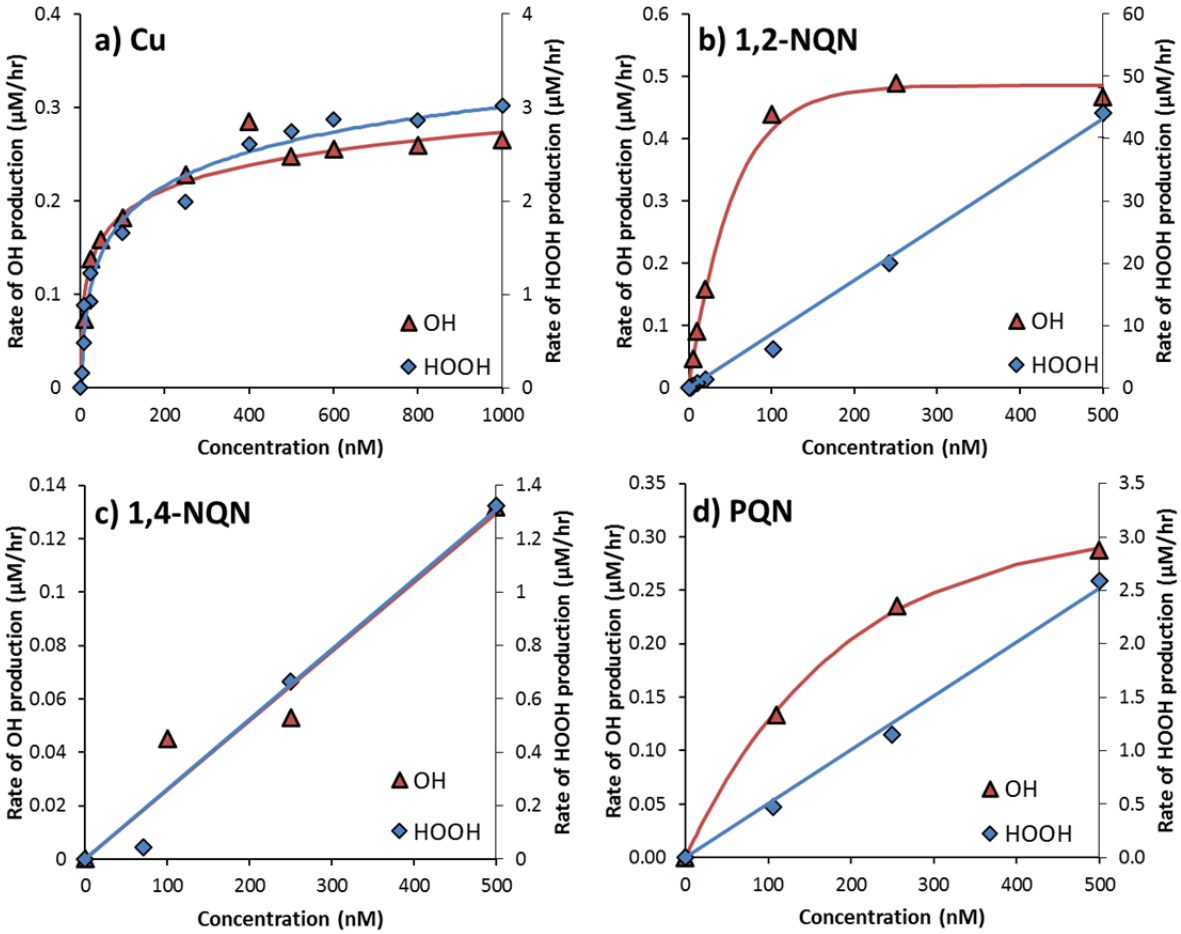

Figure S4. Rates of OH and HOOH production as a function of concentration for copper and three quinones. Fe is not included because it does not produce measurable HOOH. The HOOH axis is set to 10 times the ˙OH axis.

Table S1. Mixture Data Summary

Concentration in Mixture (nM)					Rate of ˙OH Production in Mixture (μM/hr)	Error[a] (μM/hr)	Calculated Rate of ˙OH Production from Individual Species (μM/hr)[b]	˙OH Enhancement[c] (%)
Fe	Cu	1,2-NQN	PQN	1,4-NQN				
100	250	0	0	0	0.49		0.29	169
300	250	0	0	0	0.67		0.42	159
74	173	0	0	0	0.41	1.4E-03	0.26	161
79	89	0	0	0	0.36	3.8E-03	0.23	153
242	65	0	0	0	0.46	2.2E-05	0.33	138
17	13	0	0	0	0.14	5.2E-03	0.12	119
74	49	0	0	0	0.31	1.7E-03	0.21	149
500	500	0	0	0	0.90	3.6E-02	0.58	154
1000	1000	0	0	0	1.6	5.8E-03	0.93	168
2000	1000	0	0	0	2.2		1.52	145
2000	2000	0	0	0	2.4		1.55	156
39	1022	0	3.7	0.4	0.56		0.30	187
50	0	20	0	0	0.39		0.19	208
150	0	20	0	0	0.48		0.26	186
500	0	20	0	0	0.70		0.49	143
222	549	15	0	1.1	1.2		0.52	231
442	459	2.8	3.4	0.2	1.1		0.57	185
500	500	20	0	0	1.4		0.74	190
500	0	0	500	0	1.2		0.63	189
500	500	0	500	0	1.7		0.87	190

[a] Error is the standard deviation of replicate measurements. If no error is reported then the result consists of only one measurement.

[b] The rate of ˙OH production from each species was calculated using the concentration-response curves in Table 1, then summed.

[c] 100%×(measured rate of ˙OH production / calculated rate of ˙OH production)

S4. Range and median atmospheric concentrations for active species

We have previously compiled the range and median concentrations of soluble Fe and Cu and particulate quinones [2, 3]. We use the same data to identify which species are most important for ˙OH production (Table S2). SLF concentrations were calculated assuming the ambient aerosol was sampled onto a 47 mm^2 filter at a rate of 1.465 m^3 per minute for 24 hours, then a 18.4 mm^2 section of the filter is extracted into 5.0 mL of SLF, as in Shen et al. [4].

Table S2. Typical ambient particulate concentrations of soluble metals and quinones, associated SLF concentration, and rates of HOOH and ˙OH production.

Compound	Ambient Concentration (ng/m^3)[a]			SLF Concentration (nM)			Initial rate of HOOH production from individual species (μM/hr)[b]			Rate of ˙OH production (μM/hr)		
	Low	Median	High	Low	Median	High	Low	Median	High	Low	Median	High
Soluble Fe	6.4	7.4	196	128	147	3925	0	0	0	0.09	0.10	2.2
Soluble Cu	0.88	1.9	45	15	38	783	0.82	1.29	2.9	0.11	0.15	0.26
Fe/Cu Enhancement	--	--	--	--	--	--	--	--	--	0.072	0.13	1.49
1,2-NQN	0.0018	0.017	1.1	0.013	0.35	7.8	6.5E-04	0.017	0.39	1.2E-04	0.0032	0.067
1,4-NQN	0.0025	0.11	0.71	0.017	2.2	5.0	4.2E-05	0.0053	0.012	4.5E-06	5.8E-04	0.0013
PQN	0.0012	0.32	1.8	0.0066	6.3	9.5	3.4E-05	0.033	0.050	1.1E-05	0.010	0.015

[a] Data are from [2]. Soluble metals are from [5-8], particulate-phase quinones are from [9-11].
[b] Calculated from HOOH concentration response curves for individual species from Charrier and Anastasio (2014). Does not account for Fe suppression.

S5. Potential interference by copper contamination in buffer salts

While we treat our surrogate lung fluid with chelex to remove transition metals, in some other studies this is not done. Here we examine how this could affect the apparent importance of copper as a source of oxidative potential.

The Cu content was not listed for most of the salts we used in this work, but the typical certified background Cu content for sodium chloride, sodium phosphate, and potassium phosphate is less than 0.001% by mass; this is equivalent to an upper bound of 1,440 nM Cu in our SLF. In contrast, the concentration in Cu in our SLF after chelex treatment was between 2 and 9 nM [12] and the typical median concentration of Cu in SLF extracts of ambient PM is approximately 40 nM (Supplemental table S2). Thus even if Cu contamination in the salts was one tenth of the reported upper bound value (i.e., 140 nM), the background concentration would still be 3.5 times larger than the typical concentration of Cu in the PM extracts. Background subtraction cannot correct for this background Cu problem because of the non-linear Cu-concentration response curve and because Cu and Fe synergistically produce ˙OH. The Cu concentration-response curve plateaus near 100 nM, thus a background concentration at or above 100 nM would result in a background-subtracted ˙OH production from Cu of essentially zero in the PM extract. The exact magnitude of this effect will depend strongly on the level of Cu contamination in the SLF, so we cannot speculate as to how this will affect results from ambient PM measurements using SLF that is not chelex treated. However, it is clear from the potential three-orders-of-magnitude higher level of background Cu in non-chelex-treated SLF (1,400 nM) compared to chelex-treated SLF (2 nM) that care

should be taken to understand and remove background Cu in the solutions used for ROS assays (whether OH, HOOH, DTT, or other). Chelex treatment offers a reliable, easy, and cost-effective solution to ensure low background Cu concentrations.

As an alternative approach, we attempted to use the cleanest (i.e., lowest trace metal grade) salts commercially available: Potassium phosphate monobasic (KH_2PO_4, 99.99%, Sigma-Aldrich) and sodium phosphate dibasic (Na_2HPO_4, >=99.999%, Sigma-Aldrich). In this case we observed contamination peaks in the HPLC chromatograms and atypically high blank and positive control rates for HOOH and ˙OH formation using these compounds. Thus this approach was not successful.

S6. Differences in OH production from the oxidized or reduced form of a transition metal.

In this work we use the reduced form of Fe (Fe(II)) and the oxidized form of Cu (Cu(II)). ˙OH production should not depend strongly on the oxidation state because ascorbate can rapidly cycle each of these metals between their oxidation states. Additionally, starting with reduced or oxidized forms of a metal should not significantly change ascorbate consumption or depletion. In solutions starting with Fe(II), the first OH produced requires only 2 electrons (from ascorbate) since the ferrous ion can donate an electron. Subsequent redox-cycling of that Fe (now Fe(III)) will require 3 electrons to reduce O_2 to ˙OH:

$O_2 + e^- \rightarrow {}^{\bullet}O_2^-$

${}^{\bullet}O_2^- + e^- (+2\ H^+) \rightarrow HOOH$

$HOOH + e^- \rightarrow OH + OH^-$

When starting with an Fe(III) salt, the initial production of ˙OH will require 3 electrons, as will subsequent redox-cycling of the Fe. Thus for the initial production of ˙OH, starting with Fe(III) require 50% more electrons from ascorbate than starting with Fe(II), but after the initial Fe(II) donates its electron there is no difference in the number of electrons required from ascorbate. Based on Figure 2, we estimate that each Fe(II) goes through approximately six redox cycles after it donates its initial electron. Because the difference between Fe(II) and Fe(III) will only affect the first cycling (and not the subsequent 6), we do not expect that starting with Fe(III) would make a large difference in the consumption of ascorbate. In the case of Cu(II), we believe that ascorbate is destroyed so quickly because the rates for the Cu reactions are much faster than the rates for the equivalent Fe reactions, not because we started with the oxidized form of the metal.

There is evidence for differences in ˙OH production from the two oxidation states of Fe at high concentrations, as shown in previous work, which measured OH production from 20 μM Fe(II) or Fe(III)

in an SLF containing 200 μM Asc and 300 μM Cit[13]. OH production from Fe(III) was approximately 50% higher than that from Fe(II) after 4 hours but the two cases were equal after 10 hours (Figure 1d ref. 13). Based on this it is possible that Fe(III) would exhibit a faster initial rate from 0 to 4 hours, but the result might be concentration dependent. 20 μM soluble Fe is higher than expected for extracts of atmospheric PM, and these results may not be representative of lower concentrations or our newer, four antioxidant condition.

References

1. Charrier, J. G.; Anastasio, C., Impacts of antioxidants on hydroxyl radical production from individual and mixed transition metals in a surrogate lung fluid. *Atmos. Environ.* **2011,** *45*, (40), 7555-7562.
2. Charrier, J. G.; Mcfall, A. S.; Richards-Henderson, N. K.; Anastasio, C., Hydrogen peroxide formation in a surrogate lung fluid by transition metals and quinones present in particulate matter *Env. Sci. Technol.* **2014,** *48*, (12), 7010-7017.
3. Charrier, J. G.; Anastasio, C., On dithiothreitol (DTT) as a measure of oxidative potential for ambient particles: evidence for the importance of soluble transition metals. *Atmos. Chem. Phys.* **2012,** *12*, 9321-9333.
4. Shen, H.; Barakat, A. I.; Anastasio, C., Generation of hydrogen peroxide from San Joaquin Valley particles in a cell-free solution. *Atmos. Chem. Phys.* **2011,** *11*, (2), 753-765.
5. Connell, D. P.; Winter, S. E.; Conrad, V. B.; Kim, M.; Crist, K. C., The Steubenville Comprehensive Air Monitoring Program (SCAMP): Concentrations and solubilities of $PM_{2.5}$ trace elements and their implications for source apportionment and health research. *J. Air Waste Manage. Assoc.* **2006,** *56*, (12), 1750-1766.
6. Vidrio, E.; Phuah, C. H.; Dillner, A. M.; Anastasio, C., Generation of hydroxyl radicals from ambient fine particles in a surrogate lung fluid solution. *Env. Sci. Technol.* **2009,** *43*, (3), 922-927.
7. Verma, V.; Ning, Z.; Cho, A. K.; Schauer, J. J.; Shafer, M. M.; Sioutas, C., Redox activity of urban quasi-ultrafine particles from primary and secondary sources. *Atmos. Environ.* **2009,** *43*, (40), 6360-6368.
8. Shen, H.; Anastasio, C., A comparison of hydroxyl radical and hydrogen peroxide generation in ambient particle extracts and laboratory metal solutions. *Atmos. Environ.* **2012,** *46*, 665-668.
9. Cho, A. K.; Di Stefano, E.; You, Y.; Rodriguez, C. E.; Schmitz, D. A.; Kumagai, Y.; Miguel, A. H.; Eiguren-Fernandez, A.; Kobayashi, T.; Avol, E.; Froines, J. R., Determination of four quinones in diesel exhaust particles, SRM 1649a, an atmospheric PM2.5. *Aerosol Sci. Technol.* **2004,** *38*, 68-81.
10. Delhomme, O.; Millet, M.; Herckes, P., Determination of oxygenated polycyclic aromatic hydrocarbons in atmospheric aerosol samples by liquid chromatography-tandem mass spectrometry. *Talanta* **2008,** *74*, (4), 703-710.
11. Eiguren-Fernandez, A.; Shinyashiki, M.; Schmitz, D. A.; DiStefano, E.; Hinds, W.; Kumagai, Y.; Cho, A. K.; Froines, J. R., Redox and electrophilic properties of vapor- and particle-phase components of ambient aerosols. *Environ. Res.* **2010,** *110*, (3), 207-212.
12. Charrier, J. G.; Richards-Henderson, N. K.; Bein, K. J.; Mcfall, A. S.; Wexler, A. S.; Anastasio, C., Oxidant production from source-oriented particulate matter - Part 1: Oxidative potential using the dithiothreitol (DTT) assay. *Atmos. Chem. Phys.* **2015,** *Accepted*.
13. Vidrio, E.; Jung, H.; Anastasio, C., Generation of hydroxyl radicals from dissolved transition metals in surrogate lung fluid solutions. *Atmos. Environ.* **2008,** *42* 4369-4379.